Environ. Sci. Technol. **2005**, *39,* 7731−7740

Metal Compartmentation and Speciation in a Soil Sentinel: The Earthworm, *Dendrodrilus rubidus*

JANET COTTER-HOWELLS,[†] JOHN M. CHARNOCK,[‡] CAROLE WINTERS,[§] PETER KILLE,[§] JOHN C. FRY,[§] AND A. JOHN MORGAN*[,§]

Greenpeace International Science Unit, Department of Biological Sciences, Hatherley Building, University of Exeter, Exeter EX4 4PS, United Kingdom, CCLRC Daresbury Laboratory, Warrington, Cheshire WA4 4AD, United Kingdom, and Cardiff School of Biosciences, Cardiff University, P.O. Box 915, Cardiff CF10 3TL, Wales, United Kingdom

Earthworms are well-studied organisms in ecotoxicology because of their keystone ecological status and metal-accumulating capacity. However, the direct estimation of the bioreactive fractions of accumulated metal burdens remains technically elusive. In this study we exploited two physical techniques, electron probe X-ray microanalysis (EPXMA) and X-ray absorption spectroscopy (XAS), to improve understanding of the subcellular spatial distributions, ligand affinities, and coordination chemistries of Cd, Pb and Zn in a field population of the epigeic earthworm, *Dendrodrilus rubidus*. EPXMA and XAS analyses were performed on cryopreparations to maintain compositional fidelity; EPXMA data were analyzed by multivariate statistics. XAS provided whole-worm insights; EPXMA provided in situ, subcellular data from the major metal-sequestering tissue, the chloragog. Both techniques showed that Cd is coordinated with S; the measured Cd−S bond distance in XAS suggests a metallothionein-type ligand. The mean Cd:S molar ratio (EPXMA) of 0.36 is higher than the ratio of 0.29 estimated from published biochemical data. EPXMA and XAS data also found that Ca, Pb, and Zn are predominantly bound to one or more O-donating, probably phosphate-rich, ligands. X-ray distribution maps (EPXMA) of the hepatocyte-resembling chloragocytes revealed that the O-seeking (Ca, Pb, Zn) metals and S-seeking Cd bioaccumulate in distinct organelles. Extended X-ray absorption fine structure showed that the Pb complex is not biogenic pyromorphite, although X-ray absorption near edge structure did not eliminate the possibility. XAS provided no evidence of Pb spillage from the "sequestration compartment" within *D. rubidus*. However, the correspondence of Pb with Ca and P in EPXMA is not as strong as that of Zn. This is indicative either of spillover or of a second, hitherto unidentified, sequestered-Pb pool. By exploiting the complimentary techniques of EPXMA and XAS, we are closer to describing the mechanistic link between equilibrated body burdens and biomarker responses in earthworms.

Introduction

Earthworms exert multifarious direct and indirect beneficial influences on the physical structure, nutritional status, and microbial activities of temperate soils (*1*). Their profound ecological engineering roles, albeit incompletely understood, have led to the widespread use of earthworms in terrestrial ecotoxicology and contaminated land monitoring (*2*−*4*). Biomonitoring, implicitly or explicitly, is founded on the notion that accumulated tissue burdens of environmental contaminants and their biological effects reflect the bioavailable fraction in the receptor organism's microhabitat; the accumulated burdens integrate, in time and space, the modifying interactions of abiotic and biotic variables. Total metal concentrations in a soil do not reflect the exposure of a receptor species and, therefore, cannot form the sole basis of site-specific hazard assessments or the establishment of quality standards (*5*, *6*). The concept of bioavailability has recently been extended holistically from geochemical considerations alone to encompass the fate and speciation of contaminants within the receptor organism.

The equilibrium of metal ions within the cells and tissues of a receptor organism favors the bound or sequestered state. "Free" metals can potentially pose a significant threat to a cellular system by associating nonspecifically with the amine or thiol groups of proteins, thereby compromising structural and functional integrity (*7*). Receptor organisms respond dynamically to metal intrusion. For example, essential ions, such as Zn, Cu, and Fe are usually regulated through intricate influx, efflux, and sequestration mechanisms that, in concert, maintain bioreactive metal ion levels within critical limits. Nonessential metals mimic, to greater or lesser extents, the biotic pathways of "corresponding" essential metals according to their ligand affinities and other physicochemical characteristics (*8*). Once within biological systems, the metals, whether essential or not, are bound to and relayed by chaperone molecules that control their cellular fate, in particular their delivery to, and internalization by, subcellular compartments. These compartments either act as exclusion/storage sites for essential metals or as exclusion/excretory organelles for nonessential metals. In the case of earthworms, we have previously located two metal-specific sequestration compartments (*9*) and characterized an inducible Cd-trafficking chaperone (metallothionein) (*10*) that is functionally linked with one distinct type of compartment. The structure of the metallothionein gene, whose expression correlates quantitatively with cadmium exposure (*10*), has recently been described (*11*).

Even in an invertebrate as well studied as the earthworm, the direct estimation of toxicoavailable or bioreactive metal fractions of accumulated body burdens represents a formidable technical challenge. Indirect estimates are given by quantifying the effects of metals interacting with specific genetic or molecular targets. In the words of Lanno et al. (*6*), "only organisms can determine whether a chemical is bioavailable". This is the essence of the much vaunted and widely exploited biomarker approach in ecotoxicology (*12*, *13*). Nevertheless, although biomarkers can be useful for predicting the ecotoxicological consequences of toxicant exposures, they do so at one step removed from estimating the toxicoavailability of a given metal. Toxicoavailability is a product of both metal speciation and compartmentation, parameters that have been "probed" by four generic and

* Corresponding author phone: +44 029 20875872; fax: +44 029 20874305; e-mail: morganaj1@cardiff.ac.uk.
† University of Exeter.
‡ CCLRC Daresbury Laboratory.
§ Cardiff University.

10.1021/es050648h CCC: $30.25
Published on Web 08/24/2005

TABLE 1. Composition (16 N HNO_3-extractable or -digestible; μg/g dry weight) of the Metalliferous Draethen Soil and Resident Earthworms (*D. rubidus*)[a]

	Cd	Pb	Zn	Ca	P	Cu	Fe	Ba	Mn	pH
soil	510 ± 12 (5)	16300 ± 1310 (5)	48800 ± 780 (5)	92100 ± 830 (4)	375 ± 7 (5)	140 ± 4 (5)	17920 ± 450 (5)	3350 ± 90 (5)	2000 ± 40 (5)	6.4
worm	1250 ± 210 (5)	2430 ± 320 (5)	2200 ± 510 (5)	8180 ± 800 (5)	9410 ± 350 (5)	20 ± 3 (5)	260 ± 90 (5)	100 ± 59 (5)	50 ± 25 (5)	–
BCF[b]	2.45	0.15	0.05	0.09	25.09	0.14	0.02	0.03	0.03	–

[a] The number of observations is in parentheses. Data are presented as means ± SE. [b] BCF = bioconcentration factor (i.e. whole earthworm concentration of a given element ÷ soil concentration of the given element).

relatively direct ways: (a) by fractionating tissues into detoxified-metal and nondetoxified-metal compartments (*14*), (b) by stable isotope-tracer kinetic techniques (*15*), (c) by localizing and measuring metal partitioning in structurally intact cells (*16*), and (d) by physical techniques to characterize metal−ligand coordination chemistry within tissues and cells (*17*).

The main aim of this paper was to combine approaches c and d in a complementary fashion. First, this involved using quantitative electron probe X-ray microanalysis (EPXMA) coupled with multivariate statistical analyses to improve the understanding of the spatial distributions and ligand affinities of Cd, Pb, and Zn in the main metal-sequestering cells, chloragocytes, of the earthworm, *Dendrodrilus rubidus*. Second, X-ray absorption spectroscopy (XAS) was used to determine the coordination chemistries of the metals in whole earthworms. The worms were sampled from a heavily contaminated mine-associated soil where the accumulated tissue concentrations are known to be high (*9*). Previous studies, including qualitative EPXMA, have indicated that the metals are not homogeneously distributed among the major earthworm organs and that they are discretely compartmentalized within certain tissues and cells (*9*, *18*−*20*). A similar combination of techniques was recently successfully used to determine Pb speciation and cellular distribution in a plant exposed to the metal in solution culture (*21*). In our earthworm study, all measurements were performed on cryopreparations to minimize leaching and redistribution artifacts in EPXMA (*16*) and to maintain the fidelity of metal speciation for XAS.

Methods

Earthworms and Soil. Adult (i.e. fully clitellate) earthworms, *D. rubidus* (Annelida; Oligochaeta; Lumbricidae), were collected by digging and hand-sorting soil from a disused Pb/Zn mine at Draethen, South Wales, UK (Ordnance Survey Map Ref. = ST200855). Samples of soil (from 0 to 10 cm depth; dried and sieved through a 2 mm stainless steel mesh) and whole earthworms (after 4 days depuration on moist filter paper) were, respectively, digested in boiling 16 N HNO_3 (Aristar grade; Fisher), made up to volume with ultrapure water, and analyzed for the major inorganic constituents by ICP-MS (ThermoElemental X-series) with a Cetac AS-500 autosampler. Soil pH was measured (Hanna Instruments HI9321) in 1:2 soil:water (w/v) slurries.

Electron Probe X-ray Microanalysis (EPXMA). Freshly dissected pieces (ca. 1 mm^3) of the posterior gut (i.e. intestine plus attached chloragogenous tissue) of the earthworm *D. rubidus* were hyperbarically frozen (*22*) with minimal delay in a Balzers Union HPM010 high-pressure freezer. The frozen specimens were stored in liquid N_2 prior to freeze-substitution in anhydrous ethanol (Reichert AFS; Leica, Austria) followed by low temperature embedding in Lowicryl HM20. Thin sections, nominally 600 nm thick, were cut on dry glass knives and mounted on coated titanium grids (200 mesh).

Quantitative digital X-ray distribution maps of a representative region of a chloragocyte was performed at 100 kV in a JEOL JEM-1210 transmission electron microscope interfaced with a LINK Pentafet detector (resolution = 138 eV) and LINK "ISIS" analyzer (Oxford Instruments). The maps were generated using a narrow convergent beam (diameter ~ 100 nm) and a total acquisition time of 15 h. Software based on the "Hall continuum normalization method" was used for element quantitation (*23*). Extraneous X-ray contributions emanating from the specimen holder, the support grid, and film were subtracted from the background signal. Peak deconvolution was achieved by fitting a library of peaks from pure inorganic standards. The maps were processed in two ways. First, after background correction, they were converted into single color qualitative maps. Pairs of maps were overlaid using Photoshop image processing software to determine the spatial distributions of the metals relative to the subcellular distribution patterns of the two major anions. Second, element concentration values in each pixel were exported via Microsoft Excel into MINITAB version 13.1 (Minitab Corporation Inc.) for multivariate statistical analysis.

Multivariate Statistical Analyses. Stepwise linear regression was performed to model the relationships between Cd (a S-seeking, "soft-acid" metal) or Ca (an O-seeking, "hard-acid" metal) with the other measured elements in earthworm chloragocytes. Distributional relationships between the elements were also compared by principal components analysis (PCA; MINITAB) to determine the ligand association and compartmentation of the four metal ions.

X-ray Absorption Spectroscopy (XAS). Earthworms were depurated of their gut contents by maintenance for 4 days on moist filter; the paper was changed daily. Worms were then briefly immersed in 25% ethanol and quench-frozen by immersion in liquid nitrogen. The fully hydrated frozen worms were stored at −80 °C until required.

X-ray absorption spectra at the Cd K-, Pb L(III)- and Zn K-edges were collected on Station 16.5 at the UK CLRC Daresbury SRS operating at 2GeV with an average current of 135 mA using a Si(311) double crystal monochromator and a focusing mirror that rejects harmonic contamination. Data were collected from whole earthworm material mounted on Sellotape in an aluminum sample holder, with the station operating in fluorescence mode using a 30 element solid-state Canberra detector. Experiments were performed at 77 K under vacuum and multiple scans recorded and averaged to improve the signal-to-noise ratio. The spectra were background subtracted and fitting procedures were performed in EXCURV98 (*24*) using ab initio calculated phase shifts and refining the absorber−scatterer distances and Debye−Waller factors to minimize the *R*-factor (*25*). Details of the background subtraction and fitting procedures can be found in the work of Charnock (*17*).

Results

Earthworm and Soil Composition. Metal concentrations from soil and whole, depurated worm are presented in Table 1. The main metal pollutants in this relatively calcareous mine-associated soil are Cd, Pb, and Zn. The high tissue concentrations of the three metals, even in the unlikely event

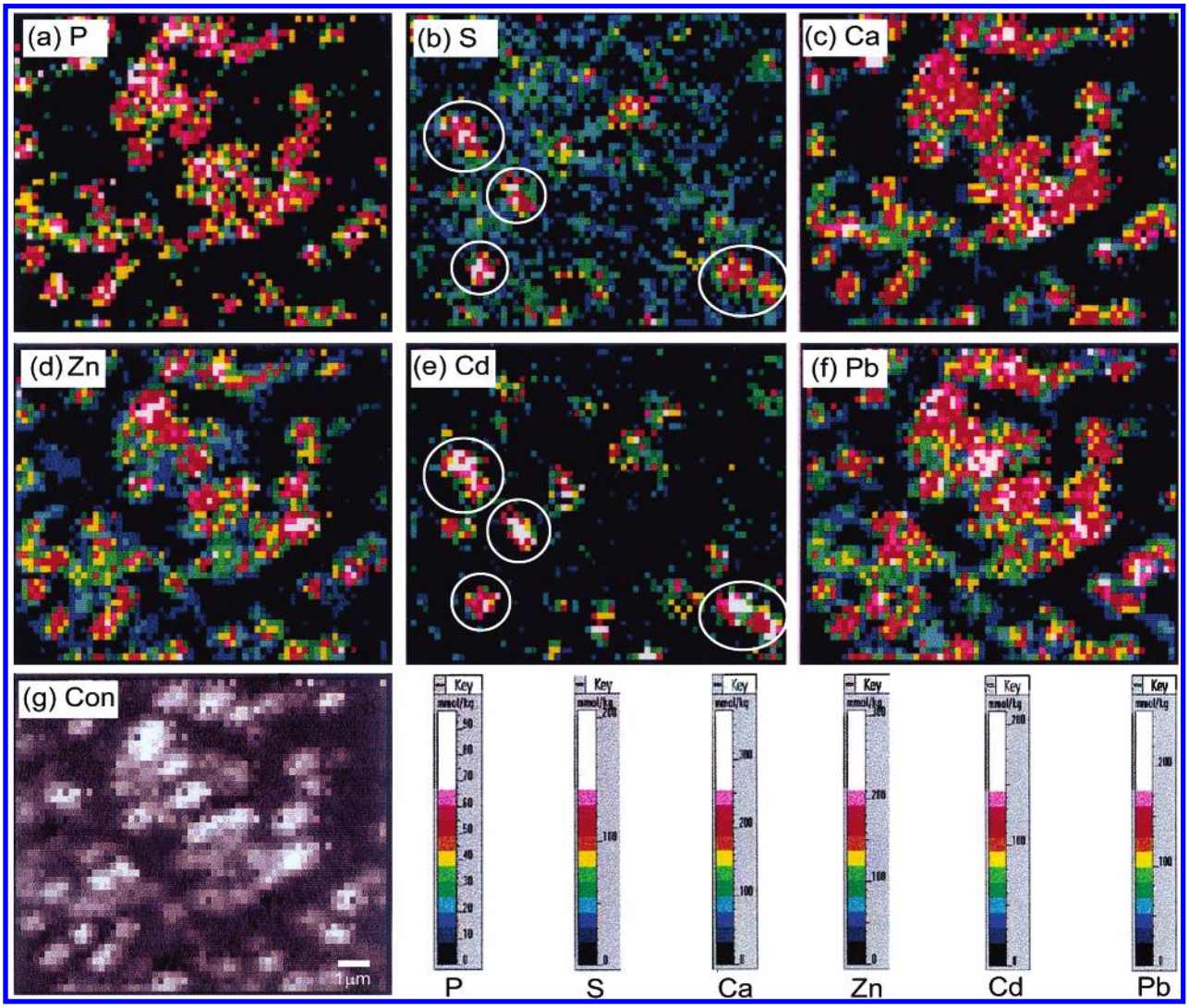

FIGURE 1. Quantitative X-ray distribution maps (a−f) for P, S, Ca, Zn, Cd, and Pb across an area of chloragogenous tissue depicted by the continuum or mass−density map (g). The concentration scales for each map are presented together; although the concentration ranges between maps differ, the pixel colors in each case are in the same descending concentration order: white > pink > red > orange > yellow > green > blue. (The concentrations correspond approximately to mmol kg^{-1} of wet weight, because tissue water was replaced during preparation with a resin of mass−density similar to that of water.) Note that the highest local Cd concentrations (e) occur in compartments with high average S contents (b) and that they are spatially distinct from the P+Ca+Zn+Pb-rich (a, c, d, f), electron-opaque (g) organelles; the perimeters of the most prominent Cd + S compartments have been outlined manually on each map for comparative purposes. Scale marker = 1 μm.

of their being homogeneously distributed among all cells and constituent subcellular compartments, indicated that the (element-related) detectable limits of EPXMA (*23*) would be exceeded, although only the Cd (and P) bioconcentration factors were above unity.

EPXMA of Chloragocytes. A continuum ("bremsstrahlung") X-ray distribution map (i.e., effectively a map of relative local mass densities) of the region of an unstained, freeze-substituted, thin cryosection of a chloragocyte that was subjected to quantitative EPXMA mapping is illustrated in Figure 1. The outlines of the characteristic, and relatively electron opaque, chloragosome granules are readily identifiable; no other compartments are discernible within this cytoplasmic field (nor could be identified on the imaging screen of the microscope prior to analysis). Quantitative X-ray distribution maps, with their accompanying color-coded concentration scales, are also presented in Figure 1. It is noteworthy that the Ca, P, Zn, and Pb "hotspots" were all centered around the chloragosome granules seen in the corresponding micrograph. The Cd and S hotspots were more-or-less contiguous with each other but spatially distinguishable from the elemental constituents of chloragosomes. Metal-discriminant partitioning and ligand binding is clarified in the binary qualitative maps (Figure 2), derived by assigning single primary colors to all the significant pixels in the individual quantitative maps. Thus, the mixing of primary colors in the overlaid paired maps indicated that the two subject elements are spatially codistributed (e.g. Ca + P; Zn + P; Pb + P; Cd + S). Conversely, the retention of primary colors indicates that the subject elements occupy different subcellular compartments (e.g. P and S, together with their respective "accompanying" metals) (Figure 2).

Stepwise regression equations (Table 2) indicate that Zn, P, and Pb are the main predictors of Ca distribution and concentration in the EPXMA map; both Cd and S are minor, negatively correlated predictors. S is, evidently, the strongest positively correlated predictor of Cd distribution, with Ca a notable, albeit negatively correlated, predictor (Table 2). The eigenvalues diagram (Figure 3) indicated that the first three components explain 93% of the variance in the EPXMA data, with most of the variance (88.3%) explained by the first two components. This justified the use of only the first three axes

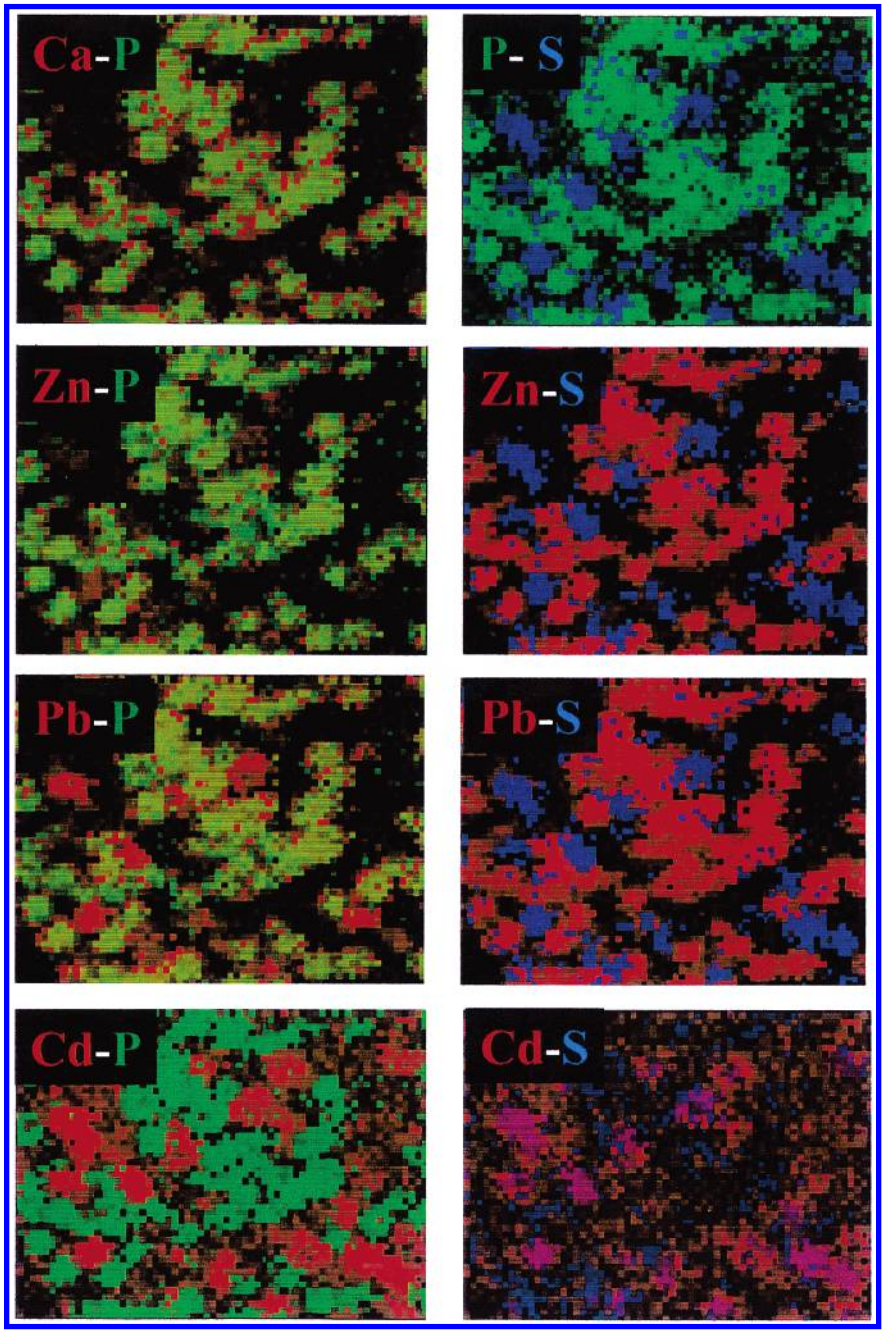

FIGURE 2. Binary (i.e. two superimposed) qualitative X-ray distribution maps created by converting the individual quantitative maps in Figure 1 into one of three pure (concentration unrelated) colors: Ca, Cd, Zn, and Pb (red), P (green), S (blue). Where the fidelities of the colors are retained in a map, the paired elements are not codistributed (P−S, Cd−P, Zn−S); where the fidelities of the colors are lost, the paired elements occupy the same subcellular compartment(s) (Ca−P, Zn−P, Pb−P, Cd−S). (The spatial resolutions of the maps and the dimensions of the mapped area can be estimated from Figure 1.)

to identify and interpret relationships in the EPXMA dataset. PCA (Figure 4a−c) confirmed the general observation (Figure 2) that Ca, Pb, and Zn are probably codistributed in a P-rich chloragocyte compartment and that Cd is codistributed with S in a compositionally distinct organelle. The partitioning of the metals and their major anionic elements is underlined by the distinct "clustering" along the negative-slope diagonal in the component 1 versus component 2 plot (Figure 4a). Pb, although tightly clustered with Ca, P, and Zn along the axes of components 1 and 3, is an outlier in the second component (Figure 4b,c). Similarly, Cd and S are separated to some extent in the first and, especially, in the third components (Figure 4a−c), probably indicating that S is an endogenous constituent of diverse biological molecules distributed in most cellular and intercellular locations.

Regression analysis (Figure 5) of Cd and S concentrations in the pixels delineating Cd-containing organelles in the EPXMA map yielded the relationship $Cd = -0.0294 + 0.425S$ ($R^2 = 0.74$; $n = 23$). The mean measured Cd:S molar ratio in these plotted pixels was 0.36 (SD = 0.127), a value slightly less than the linear regression slope of 0.43.

XAS of Whole Earthworms. The X-ray absorption spectrum comprises the X-ray absorption near edge structure (XANES), which includes the region from ca. 20 eV below the absorption edge to 50−100 eV beyond the edge, and the extended X-ray absorption fine structure (EXAFS) region, from ca. 20 eV above the edge to ca. 700 eV above the edge (Cd and Zn) or to ca. 450 eV above the edge for the Pb spectrum. The XANES spectrum is very sensitive to the coordination environment and can be used to identify the species present

TABLE 2. Summary of Stepwise Regression Analysis of EPXMA Data (n = 2816) for Ca[a] (with Cd, P, Pb, S, and Zn as predictors) and Cd[a] (with Ca, P, Pb, S, and Zn as predictors)

step	regression equations	summary statistics
	for Ca	
1	Ca = −2.551 + 1.313Zn	R^2 = 0.83, T = 117.7, P <0.001
2	Ca = −5.849 + 0.969Zn + 1.135P[b]	R^2 = 0.86, T = 25.07, P <0.001
3	Ca = −9.748 + 0.723Zn + 1.059P + 0.323Pb	R^2 = 0.87, T = 15.15, P <0.001
4	Ca = 1.996 + 0.068Zn + 0.850P + 0.466Pb − 0.336Cd	R^2 = 0.88, T = −19.31, P <0.001
5	Ca = 4.666 + 0.600Zn + 0.846P + 0.512Pb − 0.228Cd − 0.211S	R^2 = 0.89, T = −7.62, P <0.001
	for Cd	
1	Cd = −1.699 + 0.798S	R^2 = 0.40, T = 43.09, P <0.001
2	Cd = 9.812 + 0.802S − 0.157Ca	R^2 = 0.54, T = −29.65, P <0.001
3	Cd = 9.956 + 0.733S − 0.227Ca + 0.125Pb	R^2 = 0.55, T = 6.86, P <0.001
4	Cd = 10.947 + 0.729S − 0.182Ca + 0.134Pb − 0.231P	R^2 = 0.55, T = −6.30, P <0.001
5	Cd = 11.199 + 0.728S − 0.157Ca + 0.160Pb − 0.210P − 0.070Zn	R^2 = 0.56, T = −3.37, P <0.001

[a] Ca and Cd were chosen as the dependent variables because they are characteristic constituents of chloragosome granules and cadmosomes, respectively. [b] The regression equation for Ca with P as the sole predictor is Ca = 0.00801 + 3.21P (R^2 = 0.70), indicating that P has a lower association with Ca than Zn.

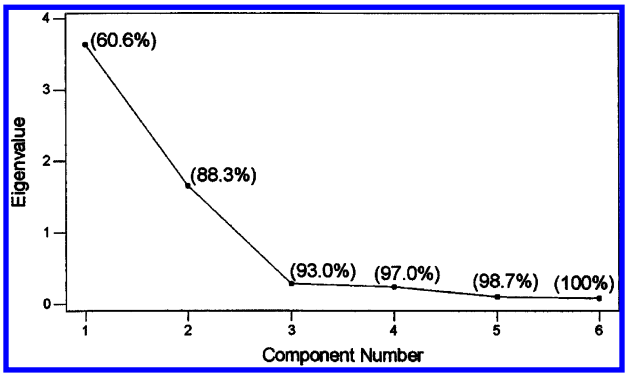

FIGURE 3. Scree plot (eigenvalue versus component number) of the EPXMA data prior to PCA.

by comparison with the XANES spectra of model compounds having known structures. The EXAFS region can be analyzed to provide distances of surrounding atoms (scatterers) from the central (Cd, Zn, or Pb) atom and also to give approximate numbers of scatterers. The Fourier transform of the EXAFS spectrum provides an approximate radial distribution profile from the central atom of shells of scatterers.

The XANES spectra for each element are shown in Figures 6a−8a together with those for model compounds. Figures 6b−8b show the best fits to the XANES spectra obtained by modeling the earthworm spectra as linear combinations of model compound spectra. Numerical parameters obtained from fitting the XANES and EXAFS spectra are given in Table 3.

The XANES spectrum for Cd (Figure 6a) shows similarities to those of CdS and two Cd−metallothioneins from Hasnain et al. (*27*), but dissimilarity with Cd−O bonded complexes, for example $CdSO_4$ or $Cd(OH)_2$. The best fit to the XANES spectra was given with the cadmium−thiol complex $[P(C_6H_5)_4]_2[Cd(S(C_6H_5))_4]$ (Table 3). The Fourier transform of the Cd EXAFS indicates a shell of scatterers at ca. 2.5 Å, and the best fit was given by coordination with four sulfur scatterers at 2.53 Å (Table 3). This Cd−S distance is in close agreement with other Cd−S distances determined experimentally by EXAFS, for example, 2.53 Å for a rabbit Zn_2-Cd_5-metallothionein (*27*), or by X-ray diffraction, for example, 2.52 Å for CdS (hawleyite and greenockite). In addition, the absence of outer shells in the EXAFS suggests light elements (which are poor scatterers and therefore give weaker EXAFS signals than heavier elements such as Cd) bonded to the sulfur in the ligand (e.g. an organic molecule) rather than a metal sulfide precipitate.

The XANES spectrum for Zn (Figure 7) gave the best fit (Table 3) with a mixture of 40−45% cysteine (S-type) binding and 55−60% phytate (O-type) binding. The Fourier transform of the zinc EXAFS spectrum clearly shows two components contributing to the inner coordination sphere, and the EXAFS was fitted as a mixture of oxygen-bound and sulfur-bound zinc species (Figure 9). The best fit found by refining the relative proportions is with 40% S and 60% O ± 10%. The Zn−S distance of 2.32 Å is typical of zinc sulfides such as sphaelerite and wurtzite and also in a range of metallothioneins (*27*). Oxygen scatterers refined to a distance of 1.95 Å, typical of tetrahedral coordination, for example in zincite, ZnO. The presence of an outer shell composed of zinc scatterers at 3.31 Å indicates the possible formation of a condensed precipitate. This distance is similar to the Zn−Zn distances in zinc oxide (3.21−3.25 Å), suggesting that the precipitate may be an oxide phase.

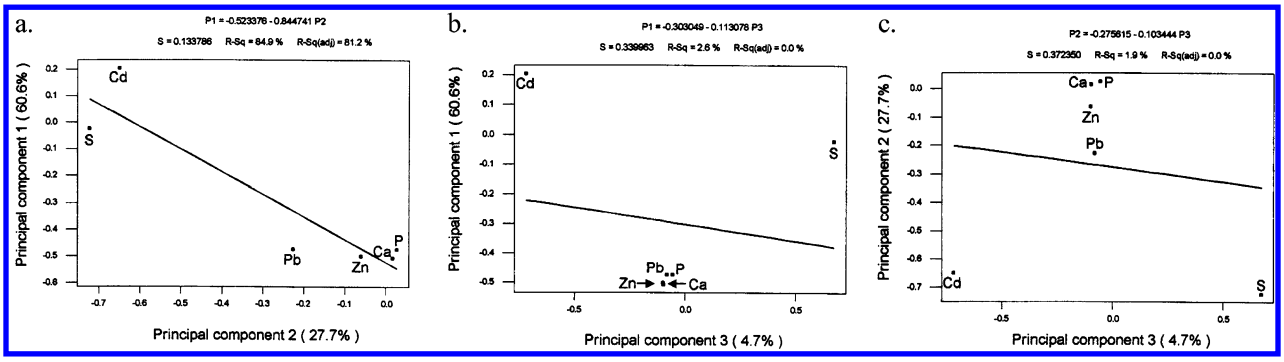

FIGURE 4. PCA plots derived from untransformed elemental concentrations derived from each pixel (n = 2816) in each of the quantitative X-ray distribution maps presented in Figure 1.

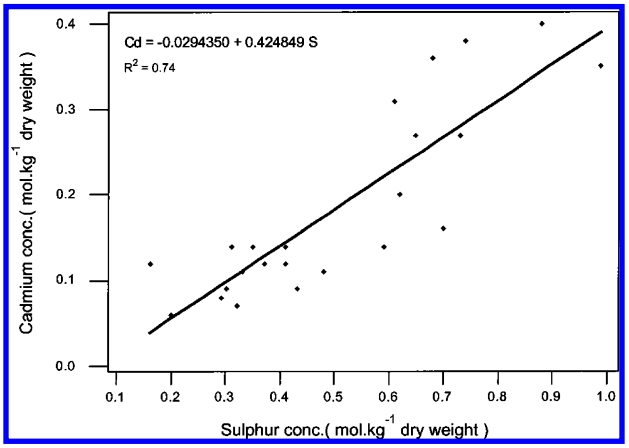

FIGURE 5. Linear regression analysis of Cd versus S concentrations (mol kg^{-1} of dry weight) in 23 corresponding pixel pairs representing three unequivocal cadmosome compartments in the quantitative EPXMA maps (see Figure 1).

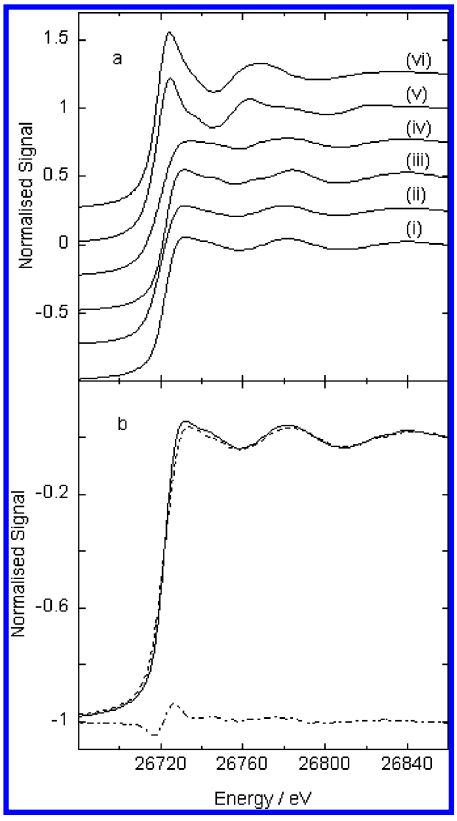

FIGURE 6. (a) XANES spectra for (i) Cd in whole earthworm, (ii) $[PPh_4]_2[Cd(SPh)_4]$, (iii) Cd_7—metallothionein, (iv) CdS, (v) $Cd(OH)_2$, and (vi) $CdSO_4$; (b) Cd in earthworm (solid line) modeled with 100% metallothionein (broken line) with residual (alternating dots and dashes).

The XANES spectrum for Pb (Figure 8) does not appear to be similar to any of the model compounds present, although the best fit was obtained with hydroxypyromorphite $[Pb_5(PO_4)_3OH]$ (Table 3). The best fit to the EXAFS was obtained with 6-fold coordination by light element(s) (N or O) with atoms at between 2.30 and 2.91 Å. Together with the absence of outer shells in the EXAFS Fourier transform, this suggests that Pb is in a very unsymmetric form, either organically bound or a disordered inorganic structure, typical of oxygen-bound lead compounds.

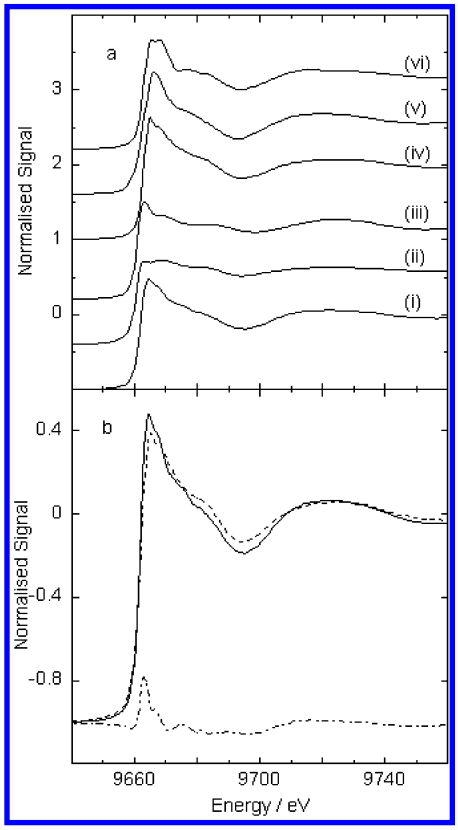

FIGURE 7. (a) XANES spectra of (i) Zn in whole earthworm, (ii) Zn—cysteine, (iii) Zn_2Cd_5—metallothionein, (iv) Zn—phytate, (v) $Zn_3(PO_4)_2$, and (vi) Zn—hopetite. (b) Zn in earthworm (solid line) modeled with 45% Zn—cysteine and 55% Zn—phytate (broken line) with residual (alternating dots and dashes).

Discussion

Before discussing the observations, it is germane to emphasize the fundamental differences and complementary capabilities of the two generic analytical techniques used in the study. Both techniques measure X-ray signals emanating from a specimen. EPXMA is essentially a cytochemical device able to detect, localize, and measure elements with high spatial resolution, on one hand, in relation to fine-structural images of the (thin) specimen, on the other hand. It is ideally suited to create multielement maps across the two-dimensional landscape of a selected cellular area, but it is incapable of detecting redox states and distinguishing between "bound" and "free" ion phases. The spatial precision of EPXMA in its transmission electron microscope mode, allied with the long acquisition times for quantitative X-ray mapping and the physical constraints on specimen size imposed by cryopreparation, conflate inevitably to give a very restricted perspective of metal compartmentation and relationships within the whole receptor organism. In the present study, EPXMA was limited to the earthworm chloragogenous tissue, a tissue noted for its prodigious metal-sequestering capacity (*20*). XAS, in comparison, is indifferent to morphological structure but highly discriminating of atomic structure, including coordination number, bond distances, and type of near-neighbors surrounding specific element centers. It, therefore, "averages" the coordination chemistries of selected metals across the tissue and cellular heterogeneities that constitute and characterize whole metazoan organisms such as earthworms. Thus, EPXMA is a compartment-defining tool and XAS a speciation-defining tool; both comment, with greater (XAS) or lesser (EPXMA) precision, on metal partitioning among ligand types.

TABLE 3. XANES and EXAFS Analyses for Whole Worms[a]

	XANES			EXAFS				
edge	% model 1	% model 2	fit index	type of scatterer	no. of scatterers	interatomic distance (Å)	$2\sigma^2$ (Å^2)	*R*-factor
Cd	100 metallothionein	–	0.00012	S	4.0	2.54	0.011	27.5
Zn	45 cysteine	55 phytate	0.00056	O	2.4	1.95	0.006	40.1
				S	1.6	2.31	0.019	
				Zn	4.0	3.31	0.036	
Pb	100 hydroxylpyromorphite	–	0.00014	O	1.0	2.30	0.018	36.4
				O	2.5	2.51	0.023	
				O	2.5	2.91	0.031	

[a] Fit index of the calculated with the experimental XANES spectra is defined as $\Sigma[(I_{obs} - I_{calc})^2]/n$, where n is the number of points in each spectrum (*26*). For EXAFS $2\sigma^2$ is the Debye–Waller-type factor and the *R*-factor indicates goodness of fit.

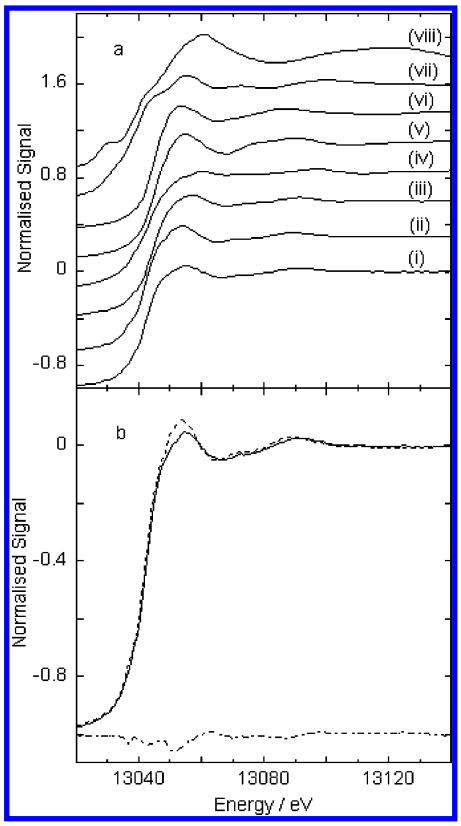

FIGURE 8. (a) XANES spectra of (i) Pb in whole earthworm, (ii) hydroxypyromorphite, (iii) pyromorphite, (iv) galena, (v) cerussite, (vi) anglesite, (vii) PbO, and (viii) PbO_2. (b) Pb in earthworm (solid line) modeled with 100% hydroxypyromorphite (broken line) with residual (alternating dots and dashes).

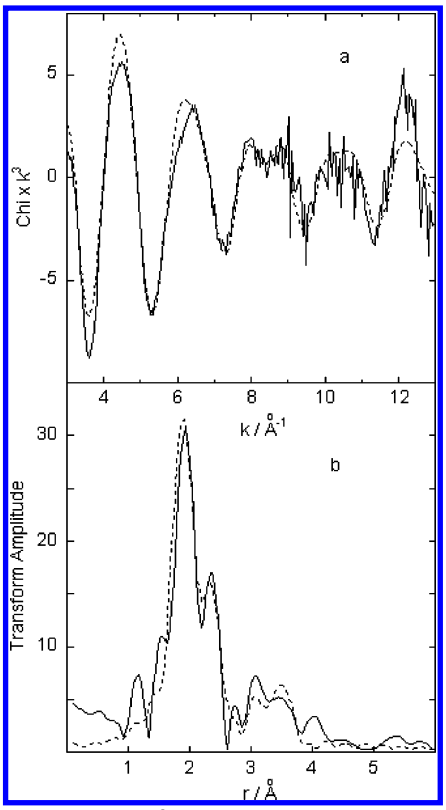

FIGURE 9. (a) Zn K-edge k^3-weighted EXAFS of whole worm (solid line) with the best fit (40% S-coordination and 60% O-coordination, broken line) and (b) corresponding phase-shifted Fourier transforms.

The data obtained by XAS provides additional insights into the elemental associations from EPXMA. Both techniques showed that Cd is coordinated with S, and the measured Cd–S bond distance in XAS suggests a metallothionein-type ligand. This is consistent with molecular genetic and immunohistochemical observations indicating that a significant proportion of the earthworm Cd burden is sequestered by cysteine-rich metallothioneins (MT) (*10*, *11*, *28*–*30*). Moreover, the glycosylation of one earthworm isoform, w-MT2, isolated from *Lumbricus rubellus* provides a mechanistic basis for the delivery and internalization of Cd-MT by a target compartment (*29*). However, EPXMA data imply the probable existence of another Cd–S phase coexistent with Cd-MT in the discrete chloragocyte organelle that has been loosely referred to as the "cadmosome" (*9*). The mean measured Cd:S molar ratio of 0.36 is higher than the calculated ratio of 0.29 [based on the reported (*29*) earthworm MT content of 21 S-containing amino acids, 20 cysteine + 1 methionine, per molecule, and 6 Cd atoms per MT molecule (*10*)]. Loading with a proton-seeking dye, Neutral Red, provides cytochemical evidence that the "cadmosome" is an acidic organelle (*30*). Mature lysosomes typically have a lower pH on the order of 4.5, but it is unlikely that Cd dissociates from MT under these conditions. Stürzenbaum et al. (*10*) showed, by in vitro proton titrations, that recombinant w-MT2 becomes 50% saturated at pH 2.8 following a steep inflection at pH ~3.5. A possible alternative fate of MT within the cadmosome is its enzymatic hydrolysis, with the precipitation of Cd with S in some form. Such a scenario allows for the continued detoxification by sequestration and entrapment of Cd within the organelle. Neither is the hypothesis inconsistent with the relatively long half-life of accumulated Cd in earthworm tissues (*31*). Moreover, the hypothesis does not entirely contradict our EXAFS observations, especially if the Cd-MT phase is dominant across all earthworm tissues. Finally, the close similarity of Cd–S(MT) and CdS bond distances gives credence to the possibility that minor Cd–S inorganic EXAFS signal may be convoluted with a stronger organic signal.

For Zn, EXAFS observations indicated binding to both S- and O-donating sites, respectively. This was not unexpected, given that Zn assumes multiple geometries with varying coordination numbers (*32*) and is considered a "borderline metal" (*33*), displaying the ligand affinities of both "hard" and "soft" metals under particular, but ill-defined, circumstances in biological systems. EXAFS detection of Zn−thiol binding in worms with a high Cd content is an important observation. It indicates that the nonessential metal, whose affinity for sulfydryls exceeds that of Zn (*34*), fails to block Zn-MT involvement in a plethora of crucial cellular activities (*35*). The segregation of the whole-earthworm Zn burden into two distinct major phases was not, however, apparent in EPXMA of chloragocytes. Chloragocytic Zn seems strongly codistributed with Ca, a strong O-seeking metal, in a P-rich compartment. Given the Zn affinity for sulfydryl groups and the Zn-inducibility of MT expression (*32*), it is surprising that Zn was not detectable by EPXMA in the so-called cadmosomes of *D. rubidus*, even though the Zn body burden was much elevated over reference values (see ref *36*). A functional interpretation may explain the apparent conflict between cell-specific EPXMA and tissue-aggregate (i.e. whole worm) EXAFS Zn observations.

Metal−thiol stability considerations dictate that Cd intrusion into cells will tend to displace Zn when the two metals compete for common ligands. The high endogenous content of Ca/P-containing organelles (*36*), so-called chloragosome granules, in chloragocytes may provide abundant Zn-sequestration sites that obviate the need for Zn-induced w-MT2 upregulation. Zinc trafficking within chloragocytes, even possibly from chloragosome stores to Zn-dependent enzymes and nonenzyme proteins, may be a function of a second MT isoform, w-MT1, that, unlike w-MT2, is not glycosylated (*29*) and has more pH-labile Cd clusters (*10*). Preventing Cd binding to w-MT1 at the expense of Zn-MT1 binding is a physiological challenge for earthworms inhabiting Cd-polluted soils. The probable unusual nature of MT gene transcription in earthworms (*11*) may contribute to this adaptive metal−metal discrimination. Moreover, the possession in chloragocytes of high-affinity w-MT2 that is internalized by cadmosomes, together with a constitutive Zn−O sequestration/storage organelle, may preserve Zn-MT1 functional capacity. Whether reduced glutathione can participate in the release and transfer of Zn from Zn−O to Zn−S (MT1) ligands in earthworms, as it is in the Zn transfer from enzymes to thionein in vertebrates (*37*), is presently unknown. While the chloragocyte may be a major target cell for Cd sequestration by w-MT2, the ubiquitous essentiality of Zn homeostasis suggests that Zn-MT1 is constitutive, albeit at relatively low expression levels, in the majority of earthworm tissues. Low, but widespread, cytosolic Zn−S concentrations would probably register in EXAFS but would be locally undetectable by EPXMA.

EPXMA indicated an association of Pb with Ca, Zn, and P in chloragosomes. XANES and EXAFS data are supportive to the extent that neither technique found Pb−S coordination. EXAFS clearly showed that the Pb complex is not crystalline pyromorphite, previously found in contaminated soils and plant roots (*38*, *39*), although the XANES profile is very similar. XAS indicated that, despite the uncertainty about the precise identity of the Pb-binding ligand, it is probably an oxygen donor or a mixture of oxygen donor ligands. The chloragosomal compartment is voluminous, but its capacity for Pb sequestration is finite, especially since it also sequesters Ca and Zn. Wallace et al. (*40*) recently hypothesized that metal tolerance in animals might reflect the ability to partition the metal among "detoxified" and "nondetoxified" compartments. A corollary of this hypothesis is that animals, metal-resistant or otherwise, overloaded with excessive metal burdens will experience a "spillover" from detoxification compartment(s) into the vulnerable nondetoxification compartments. XAS provided no evidence of Pb spillover from the metal-loaded chloragosomes of *D. rubidus*, much as Cain et al. (*14*) found no metal spillover in aquatic insects living in a polluted river. However, EPXMA of earthworm chloragocytes indicated that the correspondence of Pb with Ca and P is not as strong as that of Zn. This could either be interpreted as indicative of spillover or of a second, hitherto unidentified, sequestered-Pb pool.

In conclusion, metal bioavailability can generally be described by a "three-compartment model" of interlinked equilibria or processes (*5*). The first compartment is essentially physicochemical and related to solid-phase ↔ water partitioning in the environment surrounding soil- and sediment-dwelling organisms; the second compartment is the equilibration between the receptor organism and environmental metals at the absorptive (i.e. metal uptake) surfaces; the third compartment represents the "sequestered" ↔ "free" metal equilibrium within the tissues, cells, and body fluids of the receptor. Well-characterized, indirect chemical measurements of metal bioavailability and speciation are available to probe compartment 1 in freshwater sediments (*41*), marine sediments (*42*), and soils (*6*, *43*). Such measurements have led to the formulation, for freshwater systems, of biotic ligand models (BLM) that predict the toxic effects of a metal from measured site-specific physicochemical parameters (*44*, *45*). In principle, BLMs could be derived for earthworms despite the complexity and heterogeneity of soil matrixes, as implied by recent studies defining the Cu relationships of a collembolan (*46*) and establishing soil critical limits based on free ion concentrations (*47*, *48*), respectively. Compartment 2 relationships have received sparse direct investigations in terrestrial invertebrates (*15*), although Oste et al. (*49*) and Saxe et al. (*50*) presented models describing metal accumulation, if not uptake, by earthworms. Compartment 3 relationships are least well understood in aquatic and terrestrial biota, although they are of fundamental ecotoxicological significance because they determine the proportion of the accumulated body burden of a metal able to react either indiscriminately or specifically with biochemical targets. For this reason, the notion of "toxicoavailability" or "bioreactive fraction" has been associated with compartment 3 considerations. Furthermore, metal sequestration and speciation within a burrowing, detritivorous, receptor like the earthworm has wider ecological implications, because it may impact the trophic transference of metals (e.g. ref *40*). By exploiting, in the present study, the complimentary techniques of EPXMA and XAS we are closer to being able to develop information-based, metal-specific models of compartment 3 to, ultimately, facilitate the linkage between equilibrated body burdens and biomarker responses in earthworms.

Acknowledgments

This work was performed during the tenure of two research grants (GR/31124 and GST/02/1782) awarded by the Natural Environment Research Council to P.K. and A.J.M. We are grateful to the NERC and CCLRC for provision of beamtime at the Daresbury Synchrotron Radiation Source and would like to thank Mr. Bob Bilsborrow for his help setting up the experiment. We also thank Dr. Paul Monaghan for allowing us to use his high-pressure freezer and Dr. Iain McDonald for the ICP-MS analyses.

Literature Cited

(1) Makeshin, F. Earthworms (Lumbricidae: Oligochaeta): Important promoters of soil development and soil fertility. In *Fauna in Soil Ecosystems*; Benckiser, G., Ed.; Marcel Dekker: New York, 1997; pp 173−223.

(2) Spurgeon, D. J.; Weeks, J. M. Evaluation of factors influencing results from laboratory toxicity tests with earthworms. In *Advances in Earthworm Ecotoxicology*; Sheppard, S. C., Bembridge, J. D., Holmstrup, M., Posthuma, L., Eds.; Society of Environmental Toxicology and Chemistry (SETAC): Pensacola, FL, 1998; pp 15−25.
(3) Spurgeon, D. J. A summary of eleven years progress in earthworm ecotoxicology. *Pedobiologia* **2003**, *47*, 588−606.
(4) Van Gestel, C. A. M.; Weeks, J. M. Recommendations of the 3rd International Workshop on Earthworm Ecotoxicology, Aarhus, Denmark, August 2001. *Ecotoxicol. Environ. Saf.* **2004**, *57*, 100−105.
(5) Posthuma, L.; Notenboom, J.; De Groot, A. C.; Peijnenburg, W. J. G. M. Soil acidity as major determinant of zinc partitioning and zinc uptake in 2 oligochaete worms exposed in contaminated field soils. In *Advances in Earthworm Ecotoxicology*; Sheppard, S. C., Bembridge, J. D., Holmstrup, M., Posthuma, L., Eds.; Society of Environmental Toxicology and Chemistry (SETAC): Pensacola, FL, 1998; pp 111−127.
(6) Lanno, R.; Wells, J.; Conder, J.; Bradham, K.; Basta, N. The bioavailability of chemicals in soil for earthworms. *Ecotoxicol. Environ. Saf.* **2004**, *57*, 39−47.
(7) Finney L. A.; O'Halloran T. V. Transition metal speciation in the cell: Insights from the chemistry of metal ion receptors. *Science* **2004**, *300*, 931−936.
(8) Clarkson, T. W. Molecular and ionic mimicry of toxic metals. *Annu. Rev. Pharmacol. Toxicol.* **1993**, *32*, 545−571.
(9) Morgan, A. J.; Morris, B. The accumulation and intracellular compartmentation of cadmium, lead, zinc and calcium in two earthworm species (*Dendrobaena rubida* and *Lumbricus rubellus*) living in highly contaminated soil. *Histochemistry* **1982**, *75*, 269−285.
(10) Stürzenbaum, S. R.; Winters, C.; Galay, M.; Morgan, A. J.; Kille, P. Metal ion trafficking in earthworms: Identification of a cadmium-specific metallothionein. *J. Biol. Chem.* **2001**, *276*, 34013−34018.
(11) Stürzenbaum, S. R.; Georgiev, O.; Morgan, A. J.; Kille, P. Cadmium detoxification in earthworms: From genes to cells. *Environ. Sci. Technol.* **2004**, *38*, 6283−6289.
(12) Morgan, A. J.; Stürzenbaum, S. R.; Kille, P. A short overview of molecular biomarker strategies with particular regard to recent developments in earthworms. *Pedobiologia* **1999**, *43*, 574−584.
(13) Scott-Fordsmand, J. J.; Weeks, J. M. Biomarkers in earthworms. *Rev. Environ. Contam. Toxicol.* **2000**, *165*, 117−159.
(14) Cain, D. J.; Luoma, S. N.; Wallace, W. G. Linking metal bioaccumulation of aquatic insects to their distribution patterns in a mining-impacted river. *Environ. Toxicol. Chem.* **2004**, *23*, 1463−1473.
(15) Krebs, N. F.; Hambidge, K. M. Zinc metabolism and homeostasis: The application of tracer techniques to human zinc physiology. *BioMetals* **2001**, *14*, 397−412.
(16) Morgan, A. J.; Winters, C.; Stürzenbaum, S. X-ray microanalysis techniques. In *Electron Microscopy Methods and Protocols*; Hajibagheri, M. A. N., Ed.; Humana Press: Totowa, NJ, 2001; pp 245−276.
(17) Charnock, J. M. Biological applications of EXAFS spectroscopy. *Radiat. Phys. Chem.* **1995**, *45*, 385−391.
(18) Morgan, J. E.; Morgan, A. J. Zinc sequestration by earthworm (Annelida: Oligochaeta) chloragocytes. An in vivo investigation using fully quantitative electron probe X-ray microanalysis. *Histochemistry* **1989**, *90*, 405−411.
(19) Morgan, J. E.; Morgan, A. J. The effect of lead incorporation on the elemental composition of earthworm (Annelida, Oligochaeta) chloragosome granules. *Histochemistry* **1989**, *92*, 237−241.
(20) Morgan, A. J.; Morgan, J. E.; Turner, M.; Winters, C.; Yarwood, A. Heavy metal relationships of earthworms. In *Ecotoxicology of Metals in Invertebrates*; Dallinger, R., Rainbow, P. S., Eds.; Lewis: Boca Raton, FL, 1993; pp 333−358.
(21) Sharma, N. C.; Gardea-Torresdey, J. L.; Parsons, J.; Sahi, S. V. Chemical speciation and cellular deposition of lead in *Sesbania drummondi*. *Environ. Toxicol. Chem.* **2004**, *23*, 2068−2073.
(22) Sartori, N.; Richter, K.; Dubochet, J. Vitrification depth can be increased more than 10-fold by high-pressure freezing. *J. Microsc.* **1993**, *172*, 55−61.
(23) Hall, T. A.; Gupta, B. L. The localization and assay of chemical elements by microprobe methods. *Q. Rev. Biophys.* **1983**, *16*, 279−339.
(24) Binsted, N. CCLRC Daresbury Laboratory EXCURV98 Program, Daresbury, Warrington, UK, 1998.
(25) Binsted, N.; Strange, R. W.; Hasnain, S. S. Constrained and restrained refinement in EXAFS data analysis with curved wave theory. *Biochemistry* **1992**, *31*, 12117−12125.
(26) Salt, D. E.; Prince, R. C.; Baker, A. J. M.; Raskin, I.; Pickering, I. J. Zinc ligands in the metal hyperaccumulator *Thlaspi caerulescens* as determined using X-ray absorption spectroscopy. *Environ. Sci. Technol.* **1999**, *33*, 713−717.
(27) Hasnain, S. S.; Diakun, I.; Abrahams, I.; Ross, C. D.; Garner, I.; Bremner, I.; Vašák, M. EXAFS studies of metallothioneins. *Experientia Suppl.* **1987**, *52*, 227−236.
(28) Morgan, J. E.; Norey, C. G.; Morgan, A. J.; Kay, J. A comparison of the cadmium-binding proteins isolated from the posterior alimentary canal of the earthworms *Dendrodrilus rubidus* and *Lumbricus rubellus*. *Comp. Biochem. Physiol.* **1989**, *92C*, 15−21.
(29) Stürzenbaum, S. R.; Kille, P.; Morgan, A. J. The identification, cloning and characterization of earthworm metallothionein. *FEBS Lett.* **1998**, *431*, 437−442.
(30) Morgan, A. J.; Stürzenbaum, S. R.; Winters, C.; Grime, G. W.; Aziz, N. A.; Kille, P. Differential metallothionein expression in earthworm (*Lumbricus rubellus*) tissues. *Ecotoxicol. Environ. Saf.* **2004**, *57*, 11−19.
(31) Sheppard, S. C.; Evenden, W. G.; Cornwell, T. C. Depuration and uptake kinetics of I, Cs, Mn, Zn, and Cd by the earthworm (*Lumbricus terrestris*) in radio-spiked litter. In *Advances in Earthworm Ecotoxicology*; Sheppard, S. C., Bembridge, J. D., Holmstrup, M., Posthuma, L., Eds.; Society of Environmental Toxicology and Chemistry (SETAC): Pensacola, FL, 1998; pp 151−164.
(32) Vallee, B. L. The function of metallothioneins. *Neurochem. Int.* **1995**, *27*, 23−33.
(33) Frausto da Silva, J. J. R.;, Williams, R. J. P. *The Biological Chemistry of the Elements. The Inorganic Chemistry of Life*; Oxford University Press: Oxford, 2001.
(34) Palmiter, R. D. Regulation of metallothionein genes by heavy metals appears to be mediated by a zinc-sensitive inhibitor that interacts with a constitutively active transcription factor, MTF-1. *Proc. Natl. Acad. Sci. U.S.A.* **1994**, *91*, 1219−1223.
(35) Jacob, C.; Maret, W.; Vallee, B. L. Control of zinc transfer between thionein, metallothionein, and zinc proteins. *Proc. Natl. Acad. Sci. U.S.A.* **1998**, *95*, 3489−3494.
(36) Morgan, A. J.; Turner, M. P.; Morgan, J. E. Morphological plasticity in metal-sequestering earthworm chloragocytes: Morphometric electron microscopy provides a biomarker of exposure in field populations. *Environ. Toxicol. Chem.* **2002**, *21*, 610−618.
(37) Jiang, L. J.; Maret, W.; Vallee, B. L. The glutathione redox couple modulates zinc transfer from metallothionein to zinc-depleted sorbitol dehydrogenase. *Proc. Natl. Acad. Sci. U.S.A.* **1998**, *95*, 3483−3488.
(38) Cotter-Howells, J. E. D.; Champness, P. E.; Charnock, J. M.; Pattrick, R. A. D. Identification of pyromorphite in mine-waste contaminated soils by ATEM and EXAFS. *Eur. J. Soil Sci.* **1994**, *45*, 393−402.
(39) Cotter-Howells, J. E. D.; Champness, P. E.; Charnock, J. M. Mineralogy of lead−phosphorus grains in the roots of *Agrostis capillaris* L. by ATEM and EXAFS. *Min. Mag.* **1999**, *63*, 777−789.
(40) Wallace, W. G.; Lopez, G. R.; Levinton, J. S. Cadmium resistance in an oligochaete and its effect on cadmium trophic transfer to an omnivorous shrimp. *Mar. Ecol. Prog. Ser.* **1998**, *172*, 225−237.
(41) Meylan, S.; Behra, R.; Sigg, L. Influence of metal speciation in natural freshwater on bioaccumulation of copper and zinc in periphyton: A microcosm study. *Environ. Sci. Technol.* **2004**, *38*, 3104−3111.
(42) Almeida, C. M. R.; Mucha, A. P.; Vasconcelos, M. T. S. D. Influence of the sea rush *Juncus maritimus* on metal concentration and speciation in estuarine sediment colonized by the plant. *Environ. Sci. Technol.* **2004**, *38*, 3112−3118.
(43) Conder, J. M.; Lanno, R. P. Weak-electrolyte extractions and ion-exchange membranes as surrogate measures of cadmium, lead, and zinc bioavailability to *Eisenia fetida* in artificial soils. *Chemosphere* **2000**, *41*, 1659−1668.
(44) De Schamphelaere, K. A. C.; Janssen, C. R. Development and field validation of a biotic ligand model predicting chronic copper toxicity to *Daphnia magna*. *Environ. Toxicol. Chem.* **2004**, *23*, 1365−1375.
(45) Ryan, A. C.; Van Genderen, E. J.; Tomasso, J. R.; Klaine, S. J. Influence of natural organic matter source on copper toxicity to larval fathead minnows (*Pimephales promelas*): Implications for the biotic ligand model. *Environ. Toxicol. Chem.* **2004**, *23*, 1567−1574.

(46) Van der Zee, S. E. A. T. M.; Temminghoff, E. J. M.; Marinussen, M. P. J. C. Competition effects for copper between soil, soil solution, and yeast in a bioassay for *Folsomia candida* Willem. *Environ. Contam. Toxicol.* **2004**, *23*, 1743−1750.
(47) Lofts, S.; Spurgeon, D. J.; Svendsen, C.; Tipping, E. Deriving soil critical limits for Cu, Zn, Cd, and Pb: A method based on free ion concentrations. *Environ. Sci. Technol.* **2004**, *38*, 3623−3631.
(48) Ritchie, J. M.; Cresser, M.; Cotter-Howells, J. E. D. Toxicological response of a bioluminescent microbial assay to Zn, Pb and Cu in an artificial soil solution: Relationship with total metal concentrations and free ion activities. *Environ. Pollut.* **2001**, *114*, 129−136.
(49) Oste, L.; Dolfing, J.; Ma, W.-C.; Lexmond, T. M. Cadmium uptake by earthworms as related to the availability in the soil and the intestine. *Environ. Toxicol. Chem.* **2001**, *20*, 1785−1791
(50) Saxe, J.; Impellittori, C. A.; Peijnenburg, W. J. G. M.; Allen, H. E**.** Novel model describing trace metal concentrations in the earthworm, *Eisenia andrei*. *Environ. Sci. Technol.* **2001**, *35*, 4522−4529.

Received for review April 5, 2005. Revised manuscript received June 17, 2005. Accepted July 19, 2005.

ES050648H